Tetrahedron xxx (xxxx) xxx

Contents lists available at ScienceDirect

Tetrahedron

journal homepage: www.elsevier.com/locate/tet

Elucidation of the electrochemical behavior of phenothiazine-based polyaromatic amines

Brian M. Peterson, Luxi Shen, Gerickson J. Lopez, Cara N. Gannett, Dong Ren, Héctor D. Abruña**, Brett P. Fors*

Department of Chemistry and Chemical Biology, Baker Laboratory, Cornell University, Ithaca, NY 14853-1301, United States

ARTICLE INFO

Article history:
Received 24 April 2019
Received in revised form
24 May 2019
Accepted 29 May 2019
Available online xxx

Keywords:
Cross-coupling
Cathode
Buchwald-Hartwig Coupling
Battery
Electrochemistry

ABSTRACT

Polyarylylamines with discrete redox active groups in the polymer backbone represent a promising class of cathode materials for electrical energy storage applications. In this area, our group recently reported a set of phenothiazine-based polymers that exhibit both high capacities and power densities. In order to rationally improve the properties of these electrode materials, a fundamental understanding of their electrochemical properties is indispensable. Herein, we probe the electrochemical behavior of our phenothiazine-based systems by synthesizing small molecule analogs using C–N cross-coupling. Additionally, electropolymerization of a class of these small molecule phenothiazines yields thin films that were then characterized with an electrochemical quartz crystal microbalance. Analysis of these materials provides insights into the number of electrons accessed from each repeat unit in our polymer backbone during electrochemical cycling, as well as counter ion transport dynamics.

1. Introduction

Polymeric organic cathodes are promising alternatives to inorganic materials, owing to their high elemental abundance and their ability to tolerate fast charge rates due to facile ion transport in amorphous materials [1–3]. Many polymerization methods used to synthesize organic cathodes afford materials with insulating backbones and excess mass that does not contribute to charge storage [4–6]. This limits electron mobility to the current collector, hindering charge-discharge rates, and decreases the energy density of the organic cathode. Polyanilines are one class of materials that have the potential to overcome these limitations as they can be doped to achieve modest conductivity; however, upon discharge a continuous voltage drop is observed. We reasoned that incorporation of discrete redox active heterocycles into the polyaromatic amine backbone could circumvent the voltage drop and provide cathode materials with high energy and power densities.

Phenothiazines and phenylenediamines are two classes of molecules that display reversible redox processes at high voltages relative to Li/Li^+ [4,7–16]. Using Buchwald-Hartwig C–N cross-coupling chemistry [17,18], we envisioned that we could efficiently incorporate these units into a polyamine backbone to provide a new class of cathode materials [19,20]. Using this strategy, completely insoluble materials, **P1** and **P2**, were obtained by cross-coupling dialkylphenylene diamines (**2** and **3**) with 3,7-dibromo-10-methylphenothiazine (**1**) (Fig. 1a) in a step growth polymerization using a RuPhos-based Pd precatalyst that was developed by Buchwald and coworkers [21]. The polymers made from both phenylene diamine (**P1**) and benzidine (**P2**) showed multiple reversible redox couples. Additionally, lithium half-cells that incorporated these polymers displayed specific capacities up to 150 mAh g^{-1} and could be discharged at 120 C while maintaining 81% of their capacity. These results demonstrated that main chain polymers consisting of phenothiazine and phenylene diamine lead to materials with high capacities and high power densities.

To improve these cathode materials we need a fundamental understanding of their electrochemical properties. For both polymers **P1** and **P2**, solid state cyclic voltammetry (CV) displayed three main oxidations (−0.1, 0.3 and 0.9 V) and two smaller redox couples (0.6–0.9 V) (Fig. 1b). The presence of the latter two redox couples was unexpected. Full characterization of these two polymers was difficult due to their insolubility and inhomogeneity in chain lengths. In this manuscript, we synthesized and fully characterized small molecule analogs of these materials to gain a better

* Corresponding author.
** Corresponding author.
E-mail addresses: hda1@cornell.edu (H.D. Abruña), bpf46@cornell.edu (B.P. Fors).

https://doi.org/10.1016/j.tet.2019.05.062
0040-4020/

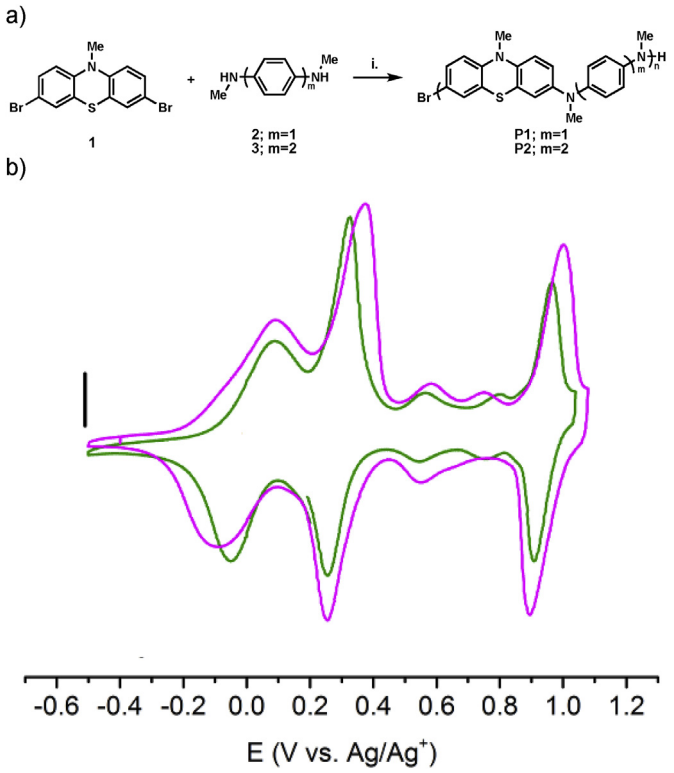

Fig. 1. a) Synthesis of **P1** and **P2**; i. NaO*t*Bu, RuPhos, RuPhos Pd G2 precatalyst, toluene, 80 °C; b) Slurry CV of **P1** (pink) and **P2** (green) in 1 M $LiPF_6$/MeCN at 20 mV s^{-1} (scale bar 25 μA).

understanding of their electrochemical behavior. Specifically, we synthesized phenothiazine based compounds that represents one and a half repeat units in the polymer backbone and fully characterize their redox processes. Further, we synthesized a small molecule analog that could be electrochemically polymerized to give **P2** on the surface of an electrode. We used such an approach to deposit films on the surface of a quartz crystal microbalance. This enables us to accurately quantify the number of oxidation events that are occurring per repeat unit on the polymer backbone, as well as characterize ionic transport and solvation dynamics.

2. Results and discussion

2.1. Synthesis of redox active small molecule

To investigate the redox properties of these polyphenothiazines, we targeted **C1**, a small molecule analog of **P1** that represents one and a half repeat units of the polymer backbone [22–26]. Using two consecutive C–N cross-coupling reactions we were able to efficiently synthesize this molecule (Fig. 2a). First, 4-bromo-*N*,*N*-dimethyl aniline (**4**) was coupled with methyl amine using a catalyst system developed by Buchwald and coworkers to yield the phenylene diamine **5** [27,28]. A second cross-coupling between **1** with **5,** using a RuPhos-based Pd catalyst, gives **C1** in 63% yield [29,30]. The small molecule analog, **C1**, quickly oxidizes in air; therefore, **C1** was kept under nitrogen and electrochemical studies were conducted in deoxygenated solvents.

The CV of **C1** shows five reversible redox couples between −0.5 and 1.1 V vs. Ag/Ag^+(Fig. 2b and c). The first four redox couples appear reversible, while the fifth oxidation is followed by adsorption onto the electrode. This degree of redox activity is rarely observed in soluble organic molecules. As **C1** is comprised of 1.5 repeat units of **P1**, four to five redox events were expected. The presence of five reversible redox events shows that the structural units of **P1** are indeed stable in a highly oxidized state.

The spectrochemical signature of **C1** in each oxidation state was characterized *in situ* (Fig. 2d). We observed that the neutral and monocationic states exhibit distinct electronic absorption spectra, while similar absorption behavior was observed between the di- and tricationic states and between the tetra- and pentacationic states. In the UV region, distinct sets of electronic absorptions were observed in the neutral state, distinguished by absorptions at 263 and 328 nm, and in the monocationic state, at 268 and 288 nm. In the 400–800 nm region, di- and tricationic states show absorptions at 588 nm, while tetra- and pentacationic states exhibit absorptions at 817 nm.

2.2. Electropolymerization of thin-film P2-TF

When analyzing **P1** in a Li half-cell, we observed good agreement between theoretical and experimental capacity, if only two electrons are exchanged during charge and discharge. To further support our observation that we could efficiently access the first two redox couples of our polymers in the Li half-cells, we set out to quantitatively determine the number of electrons involved in each redox event for our materials. We hypothesized that we could electropolymerize a thin film of **P2** on a quartz crystal microbalance electrode, which would allow us to accurately quantify the number of counterions transported in and out of the film when oxidized and reduced. This experiment would give us evidence for the number of electrons accessed from each repeat unit during cycling.

We proposed that we could deposit **P2** as a thin film (**P2-TF**) on an electrode surface through the electrochemical oxidative step growth polymerization of monomer **C2** (Fig. 3b), based on the fact that the electrochemical dimerization of anilines to benzidine is a well-studied and highly efficient reaction [14,31]. To test our strategy, we synthesized monomer **C2** in 66% yield by coupling N-methylaniline with **1** (Fig. 3a). **C2** exhibited two highly reversible redox couples at 0.0 and 0.3 V (Fig. 3b and c) and efficiently polymerized into a thin film upon a third oxidation at 1.3 V, which can be observed by an increase in current in subsequent cycles. In dichloromethane (DCM), adsorptive behavior is observed at high concentration, and deposition on the electrode can be monitored during sequential scans (Fig. 3d). The coupling reaction can also be monitored spectroscopically (Fig. 3e). The neutral, 1^+ and 2^+ states of the monomer can be clearly seen as the potential of the electrode is swept from −0.4–1.2 V. The coupled species between two tricationic **C2** species ($\mathbf{C2}^{3+}$) is observed when sweeping the potential in the reverse direction between 1.2 and 0.8 V, which is followed by polymer deposition on the electrode surface. Sweeping the potential to more negative values, any uncoupled $\mathbf{C2}^{3+}$ is reduced to the dication state, which can be observed between 0.8 and 0.2 V. Once the potential of electrode is swept past 0.2 V, the characteristic spectral peak of $\mathbf{C2}^{2+}$ at approximately 850 nm recedes. Continuing to sweep between 0.2 and −0.4 V, the spectral signature of the 1^+ oxidation state is observed before being reduced to neutral **C2** at −0.2 V.

2.3. Electrochemical quartz crystal microbalance

With efficient conditions for the electrochemical formation of **P2-TF**, we set out to deposit a thin film on a quartz crystal microbalance electrode to perform electrochemical quartz crystal microbalance (EQCM) analysis during cycling [32]. EQCM enables monitoring of the mass changes associated with ion movement and viscoelastic changes in a thin-film during electrochemical processes [33–35]. Numerous studies have employed this method to

Please cite this article as: B.M. Peterson et al., Elucidation of the electrochemical behavior of phenothiazine-based polyaromatic amines, Tetrahedron, https://doi.org/10.1016/j.tet.2019.05.062

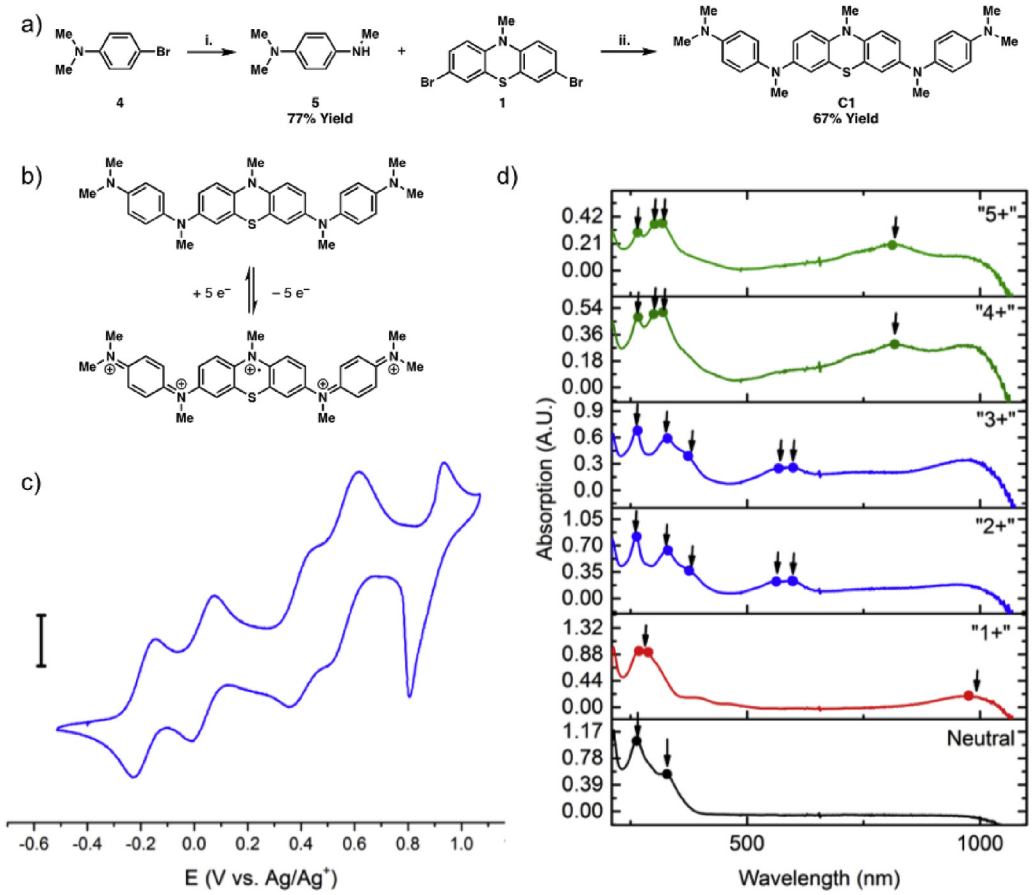

Fig. 2. a) Synthesis of **C1**; i. NaO*t*Bu, BrettPhos, BrettPhos Pd G3 precatalyst, methylamine, *t*BuOH, 80 °C; ii. NaO*t*Bu, RuPhos, RuPhos Pd G2 precatalyst, dioxane, 80 °C; b) Oxidation of **C1** to the pentacationic state; c) CV of 0.5 mM **C1** in 0.1 M TBAP in 1:1 MeCN/DCM at 20 mV s^{-1} (scale bar 5 μA); d) UV−Visible absorption spectra of **C1** in each redox state; arrows indicate the major absorptions.

elucidate transport dynamics in thin-film materials. To probe the redox mechanisms of **P2-TF** we employed EQCM to monitor the anion flux into the film as the polymer was oxidized in electrolyte solution. This enables us to determine the approximate number of electrons exchanged per repeat unit in **P2-TF**, and by extension **P1**, and **P2**.

The EQCM experiment was divided into two parts: electropolymerization and film cycling (Fig. 4a). Polymer film mass was established by the frequency change of the QCM electrode in solution, before and after electropolymerization. Frequency and mass changes are minimal during the first two redox couples. However, when the potential of the gold electrode was scanned to 1.10 V, a sudden and large decrease in frequency, and increase in mass, associated with film deposition were observed, as seen in Fig. 4a through 1250 s. Typically, twenty cycles of electropolymerization yielded a film-thickness of 40−50 nm, as measured by contact profilometry. This yielded a mass loading in the range of a few μg cm^{-2}.

Upon completion of electropolymerization, **P2-TF** was subjected to cycling in blank electrolyte solution containing no monomer. During film cycling, frequency and mass changes are attributed to anion movement into and out of the polymer film, between 1250 and 2500 s in Fig. 4a. Upon cycling the potential of the electrode between −0.6−0.8 V the frequency decreased, corresponding to an increase in mass, which was attributed to an influx of charge compensating perchlorate ions into the polymer film (Fig. 4b). During the reverse scan, an increase in frequency, corresponding to a decrease in mass, is observed as anions diffuse out of **P2-TF**. Simultaneous resistance measurements indicate no significant changes in the viscoelastic properties during potential cycling. This confirms the rigid film nature of the **P2-TF**, and allows for the direct application of the Sauerbrey equation, which correlates frequency changes to a change in mass on the QCM electrode.

Only the first two redox couples near 0.0 and 0.3 V could be studied, since the electrochemical stability of the gold electrode of the QCM does not allow potential sweeps beyond 0.8 V vs. Ag/Ag^{+}. When the thin film is oxidized to the dication, approximately 0.8 counterions diffuse into the thin film, which is in contrast to our expectation that two counterions would be brought in during cycling to account for the two redox couples in the CV (Fig. 4d).

We hypothesized that this discrepancy in the capacity of our Li half-cells and EQCM studies could be explained by two scenarios: the film is not fully accessed by ions, leading to an underestimation of anions transported in, or a portion of the film was dissolving away while the electrode was washed. Film cycling in the presence of ferrocene, as a redox shuttle, could aid in unclogging any electronically or ionically isolated portions of film. However, no sign of unclogging or improvement of film accessibility was observed (Fig. S11). Therefore, we hypothesized that if the film was indeed washing away when rinsed with acetone after the film was deposited, incorporation of a cross-linker could improve the polymer's adherence to the gold electrode (Fig. 4c). It is important to mention that we observed similar behavior in our Li half-cells. The linear polymer of **P1** showed significant capacity fade after every

Please cite this article as: B.M. Peterson et al., Elucidation of the electrochemical behavior of phenothiazine-based polyaromatic amines, Tetrahedron, https://doi.org/10.1016/j.tet.2019.05.062

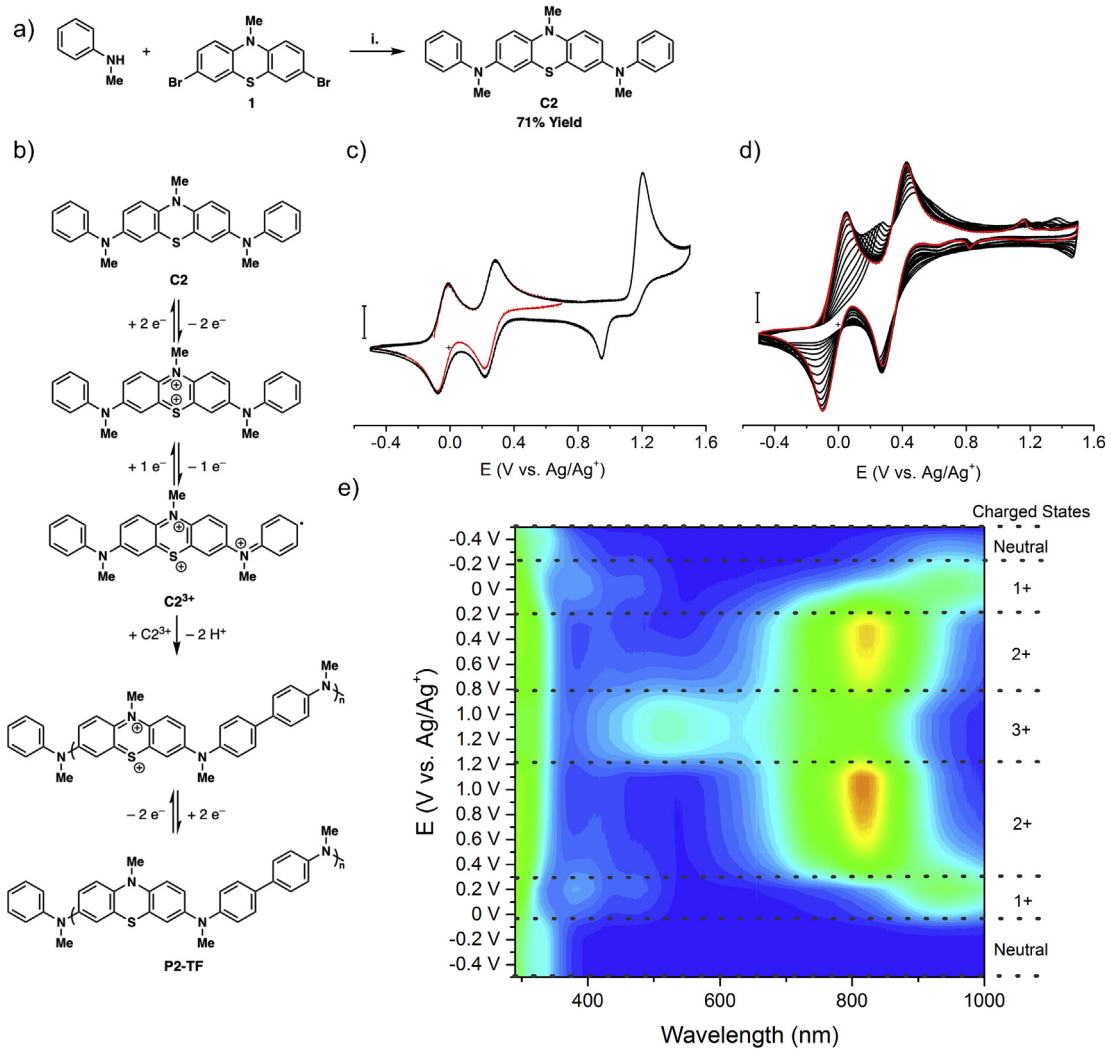

Fig. 3. a) Synthesis of **C2**; i. NaO*t*Bu, RuPhos, RuPhos Pd G2 precatalyst, dioxane, 80 °C; b) Mechanism of the electropolymerization of **C2** and redox states of **P2-TF**; c) CV profile of **C2** at 0.5 mM in 0.1 M TBAP in MeCN (scale bar 10 μA); small window (red) vs. full window (black); d) Electropolymerization of **C2** at 10 mM in 1 M TBAP in DCM at 50 mV s^{-1} on a glassy carbon electrode (scale bar 20 μA); first scan (red) and subsequent scans (black); e) UV–Vis spectra of **C2** in electrolyte solution during potential sweeping from −0.4–1.2 V.

charging cycle due to dissolution of the active material. In our initial coin cell study, we demonstrated that cross-linking of the polymer film mitigated dissolution of the polymers.

Electropolymerization of **C2** with varying amounts of cross-linker **C3** to cross-link the thin film in the EQCM experiment could prevent dissolution of the thin film during washing. No difference was observed during electropolymerization or film cycling, as the addition of the cross-linker did not alter the polymer's redox activity (only a butyl-chain differentiates the cross-linker from the monomer, as shown in Fig. 4c). With incremental addition of cross-linker **C3** to the electropolymerization solution, the number of electrons exchanged increased to 2.17 per repeating unit at 10 mol% **C3**. At higher loadings of **C3** (20 mol%), a decrease in electrons exchanged per repeat unit was observed. This decrease at higher cross-linker content is likely due to transport limitations arising from the highly cross-linked network (Fig. 4d). These experiments are in good agreement with our coin cell studies where we found that the optimal cathode material contained 10% cross-linker. Moreover, these results suggest that two electrons are exchanged per repeat unit during potential sweeps through the first two redox couples. This is in excellent agreement with our previous study which showed an experimental capacity of 150 mAh g^{-1} in agreement with the theoretical capacity for two electron energy storage in **P1** (152 mAh g^{-1}).

3. Conclusion

This study provides a thorough and comprehensive analysis of the electrochemical and spectrochemical behavior of two charge storing polymers synthesized by palladium-catalyzed C–N cross-coupling reactions. The investigation of the small molecule analog **C1**, provided confidence that the charge storing units in **P1** are stable in all accessible oxidation states. Analysis of the core structure of **P2** in a thin film provided evidence that nearly quantitative oxidation of the first two redox couples contributes to the experimental capacity observed in these phenothiazine based polyaromatic amines. The electropolymerization of cross-linked **P2-TF** was analyzed by EQCM and cycling the potential between the first two redox processes showed that 2.18 electrons are accessed per repeat unit. Through the analysis of small molecule and thin film analogs, the spectrochemical and electrochemical properties of a series of redox active polymer cathode materials were probed.

Please cite this article as: B.M. Peterson et al., Elucidation of the electrochemical behavior of phenothiazine-based polyaromatic amines, Tetrahedron, https://doi.org/10.1016/j.tet.2019.05.062

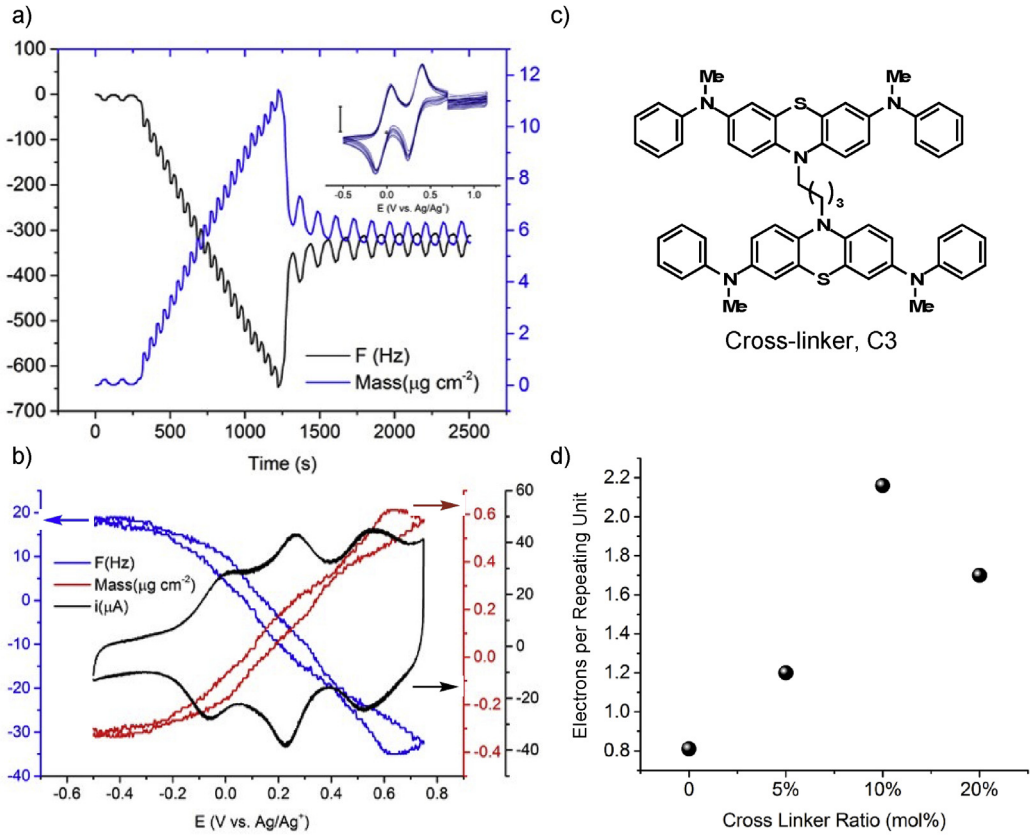

Fig. 4. a) Frequency and mass changes during electropolymerization of **C2** on a QCM Au electrode. Inset shows the CV profile during the electropolymerization, polymerization was achieved by cycling between 0.7 and 1.15 V to accelerate film deposition (10 mM **C2** in 1 M TBAP/DCM, scale bar: 500 μA); b) The simultaneous change in frequency and mass during cycling of **P2-TF** in fresh electrolyte, 0.1 M TBAP/MeCN at 20 mVs^{-1}; c) Chemical structure of cross-linker **C3**; d) The number of electrons exchanged during film cycling as a function of the amount of **C3** present during electropolymerization.

4. Experimental

4.1. General methods

Toluene, DCM, and THF were purchased from J.T. Baker and were purified by vigorous purging with argon for 2 h, followed by passing through two packed columns of neutral alumina under argon pressure. BrettPhos (96%), BrettPhos Pd G3 (95%), RuPhos (95%), RuPhos Pd G2, sodium *tert*-butoxide (NaO*t*Bu), potassium *tert*-butoxide (KO*t*Bu), anhydrous hydrazine, 4-bromo-*N,N′*-dimethylaniline (97%), and methylaniline were purchased from Sigma Aldrich and used as received. 1,4-dibromobutane (99%), phenothiazine (98%+), iodomethane (99.5%), and methylamine (2 M in THF) were purchased from Alfa Aesar and used as received. Anhydrous magnesium sulfate ($MgSO_4$) was purchased from EMD Chemicals. *N*-Bromosuccinimide was purchased from Oakwood Chemicals and recrystallized from DI water before use as a brominating agent. Sodium sulfite (Na_2SO_3) was purchased from Fischer Scientific and used as received. Tetrabutylammonium perchlorate (TBAP) was purchased from TCI (>98%), and recrystallized from ethyl acetate (EtOAc) three times to obtain white crystals. Acetonitrile (MeCN) was purchased from Fisher (ACS grade) dried over activated 4 Å molecular sieves. 1-Methyl-2-pyrrolidinone (NMP, anhydrous, 99.5%) was purchased from Sigma Aldrich and used as received.

Nuclear magnetic resonance (NMR) spectra were recorded on a Mercury 300 MHz, a Varian 400 MHz or a Bruker 500 MHz. Cyclic voltammetric analysis on glassy carbon electrodes were performed on a Hokuto Denko HABF1050m potentiostat/galvanostat controlled by LabView program. UV–vis spectroscopy experiments were carried out using an Agilent/HP 8453 UV–visible spectroscopy system. Frequency, mass, and resistance data were measured on a Model QCM 200 Quartz Crystal Microbalance Digital Controller from Stanford Research Systems and processed by a SRS LabVIEW program. The temperature of the electrochemical system was controlled by a Fisher Scientific thermostat (Model No. 9101). 5 MHz AT-cut quartz crystals sputtered with gold were obtained from Maxtek, with a front electrode area of 1.37 cm^2 and used for EQCM experiments. Polymer P1, P2 and small molecules 10-methylphenothiazine, 3,7-dibromo-10-methylphenothiazine (**1**), *N,N′*-dimethyl-*p*-phenylenediamine (**2**), *N,N′*-dimethylbenzidine (**3**), 1,4-bis(3,7-dibromo-10*H*-phenothiazin-10-yl)butane were synthesized by literature procedures [21].

4.1.1. *N,N,N′-trimethyl-p-phenylenediamine (**5**)*

4-Bromo-*N,N*-dimethylaniline (600 mg, 3 mmol, 1 equiv), NaO*t*Bu (432.5 mg, 4.5 mmol, 1.5 equiv), BrettPhos (16.1 mg, 0.03 mmol, 0.01 equiv), BrettPhos Pd G3 (27.21 mg, 0.03 mmol, 0.01 equiv), and a magnetic stir bar were charged to a flame dried, 20 mL reaction tube and sealed with a Teflon cap. A nitrogen atmosphere was established and methylamine (2M in THF) (3 mL, 6 mmol, 2 equiv) and *tert*-butanol (6 mL) were added. The reaction was stirred at 80 °C for 7 h. The reaction mixture was extracted into ethyl acetate (EtOAc) and washed with water. The organic layer was dried with $MgSO_4$ and concentrated. Purification by silica column chromatography (4:6 EtOAc:Hexanes) yielded 346 mg (77% yield) of the desired product. ^{1}H NMR ($CDCl_3$, 500 MHz): δ 6.77 (d, 2H), 6.62 (d, 2H), 2.83 (s, 6H), 2.81 (s, 3H); ^{13}C NMR ($CDCl_3$, 126 MHz): δ 144.15, 142.06, 115.99, 113.89, 42.36, 31.74; IR (ATR, cm^{-1}): 3397, 3022,

Please cite this article as: B.M. Peterson et al., Elucidation of the electrochemical behavior of phenothiazine-based polyaromatic amines, Tetrahedron, https://doi.org/10.1016/j.tet.2019.05.062

2941, 2873, 2799, 1520, 1476, 1447, 1304, 815.

4.1.2. $N^1,N^{1'}$-(10-methyl-10H-phenothiazine-3,7-diyl)bis(N^1,N^4,N^4-trimethylbenzene-1,4-diamine) (**C1**)

3,7-Dibromo-N-methylphenothiazine (93 mg, 0.25 mmol, 1 equiv), N, N, N′-trimethyl-1,4-diaminobenzene (115 mg, 0.75 mmol, 3 equiv), NaO*t*Bu (75 mg, 0.75 mmol, 3 equiv), RuPhos (2.3 mg, 2.5 μmol, 0.01 equiv), RuPhos Pd G2 (3.8 mg, 2.5 μmol, 0.01 equiv), and a magnetic stir bar were charged to a flame dried, 20 mL reaction tube and sealed with a Teflon cap. A nitrogen atmosphere was established and dioxane (2 mL) was added via syringe. The reaction was stirred at 80 °C for 16 h. After cooling, the reaction was diluted with EtOAc and washed with DI water. The organic layer was dried with $MgSO_4$ and concentrated. Purification by silica column chromatography (2:3 EtOAc:Hexanes) yielded 80 mg (63%) of the desired product. Hydrazine was added to NMR to prevent oxidation of product. ^{1}H NMR (500 MHz, $CDCl_3$) δ 6.95 (d, $J = 8.9$ Hz, 4H), 6.71 (d, $J = 8.9$ Hz, 4H), 6.68 (t, $J = 1.5$ Hz, 2H), 6.64 (d, $J = 1.6$ Hz, 4H), 3.27 (s, 3H), 3.16 (s, 6H), 2.91 (s, 12H); ^{13}C NMR (126 MHz, $CDCl_3$) δ 147.1, 145.6, 139.8, 138.9, 124.4, 124.0, 116.3, 116.1, 114.0, 113.9, 41.2, 40.9, 35.1; IR (ATR, cm^{-1}): 2933, 2821, 2781, 1515, 1485, 1450, 1326, 1259, 820; HRMS (DART): *m/z* calc'd for $(M + H)^+$ $[C_{31}H_{36}N_5S]^+$: 510.2691, found 510.2693.

4.1.3. N3,N7-10-trimethyl-N3,N7-diphenyl-10H-phenothiazine-3,7-diamine (**C2**)

1 (743 mg, 2 mmol, 1 equiv), RuPhos ligand (9.7 mg, 0.02 mmol, 0.01 equiv), RuPhos Pd G2 precatalyst (15.5 mg, 0.02 mmol, 0.01 equiv), NaO*t*Bu (575 mg, 6 mmol, 3 equiv), and a magnetic stir bar were charged to a flame dried, 20 mL reaction tube and sealed with a Teflon cap. A nitrogen atmosphere was established and N-Methylaniline (0.44 mL, 4 mmol, 2 equiv) and dioxane (2 mL) were added via syringe. The reaction was stirred at 80 °C for 16 h. After cooling, the reaction was diluted with DCM and washed with DI water three times. The organic layer was dried with $MgSO_4$ and concentrated. Purification by silica column chromatography (1:1 DCM:Hexanes) yielded 562 mg (66% yield) of the desired product. ^{1}H NMR (500 MHz, C_6D_6) δ 7.14 (m, 4H), 6.95 (d, $J = 2.5$ Hz, 4H), 6.84 (d, $J = 8.3$ Hz, 4H), 6.83–6.78 (m, 4H), 6.33 (d, $J = 8.6$ Hz, 2H), 2.87 (s, 6H), 2.74 (s, 3H); ^{13}C NMR (125 MHz, C_6D_6) δ 149.9, 144.5, 142.2, 129.4, 125.0, 123.2, 123.1, 119.8, 117.6, 114.7, 40.2, 35.0; HRMS (DART): *m/z* calc'd for $(M + H)^+$ $[C_{27}H_{26}N_3S]^+$: 424.1847, found 424.1845.

4.1.4. 10,10'-(butane-1,4-diyl)bis(N^3,N^7-dimethyl-N^3,N^7-diphenyl-10H-phenothiazine-3,7-diamine) (**C3**)

1,4-bis(3,7-dibromo-10*H*-phenothiazin-10-yl)butane (115 mg, 0.15 mmol, 1 equiv), NaO*t*Bu (96.1 mg, 1 mmol, 6.6 equiv), RuPhos (1.4 mg, 0.003 mmol, 0.02 equiv), RuPhos Pd G2 (2.3 mg, 0.003 mmol, 0.02 equiv), and a magnetic stir bar were charged to a flame dried, 20 mL reaction tube and sealed with a Teflon cap. A nitrogen atmosphere was established and methylaniline (0.1 mL, 0.9 mmol, 6 equiv) and dioxane (1 mL) were added via syringe. The reaction was stirred at 80 °C overnight. The reaction was quenched with Na_2SO_3 and stirred for 30 min. Product was extracted into DCM and dried with $MgSO_4$. The organic layer was concentrated and dried under vacuum. The product was isolated by recrystallization from benzene yielding 78 mg (59% yield) of light green powder. ^{1}H NMR (500 MHz, C_6D_6) δ 7.11 (dd, $J = 8.7, 7.2$ Hz, 8H), 6.97 (d, $J = 2.5$ Hz, 4H), 6.87–6.77 (m, 16H), 6.46 (d, $J = 8.7$ Hz, 4H), 3.39 (m, 4H), 2.86 (s, 12H), 1.71 (m, 4H); ^{13}C NMR (125 MHz, C_6D_6) δ 149.4, 144.3, 141.0, 129.1, 126.4, 122.6, 122.4, 119.7, 117.7, 116.0, 46.4, 39.9, 24.0; IR (ATR, cm^{-1}): 3053, 2919, 2848, 2805, 1593, 1493, 1455, 1250, 1153, 1129, 1088, 748; HRMS (DART): *m/z* calc'd for $(M + H)^+$ $[C_{56}H_{53}N_6S_2]^+$: 873.3773, found 873.3787.

Dedication

In honor of Prof. Stephen L Buchwald for his mentorship and leadership in the field of organic chemistry.

Acknowledgements

This work was primarily funded by a grant to the Cornell Center for Materials Research from the NSF MRSEC program (DMR-1719875). B.P.F. thanks 3M for a Non-Tenured Faculty Award and the Sloan Foundation for the Sloan Research Fellowship.

Appendix A. Supplementary data

Supplementary data to this article can be found online at https://doi.org/10.1016/j.tet.2019.05.062.

References

[1] Q. Zhao, C. Guo, Y. Lu, L. Liu, J. Liang, J. Chen, Ind. Eng. Chem. Res. 55 (2016) 5795.
[2] T.B. Schon, B.T. McAllister, P.-F. Li, D.S. Seferos, Chem. Soc. Rev. 45 (2016) 6345.
[3] P. Novák, K. Müller, K.S.V. Santhanam, O. Haas, Chem. Rev. 97 (1997) 207.
[4] S. Conte, G.G. Rodriguez-Calero, S.E. Burkhardt, M.A. Lowe, H.D. Abruña, RSC Adv. 3 (2013) 1957.
[5] Y. Liang, Z. Tao, J. Chen, Adv. Energy Mater. 2 (2012) 742.
[6] S. Muench, A. Wild, C. Friebe, B. Häupler, T. Janoschka, U.S. Schubert, Chem. Rev. 116 (2016) 9438.
[7] A.A. Golriz, T. Suga, H. Nishide, R. Berger, J.S. Gutmann, RSC Adv. 5 (2015) 22947.
[8] M. Kolek, F. Otteny, P. Schmidt, C. Mück-Lichtenfeld, C. Einholz, J. Becking, E. Schleicher, M. Winter, P. Beiker, B. Esser, Energy Environ. Sci. 10 (2017) 2334.
[9] T. Godet-Bar, J.-C. Lepretre, O. Le Bacq, J.-Y. Sanchez, A. Deronzier, A. Pasturel, Phys. Chem. Chem. Phys. 17 (2015) 25283.
[10] J.A. Kowalski, M.D. Casselman, A.P. Kaur, J.D. Milshtein, C.F. Elliot, S. Modekrutti, N.H. Attanayake, N. Zhang, S.R. Parkin, C. Risko, F.R. Brushett, S.A. Odom, J. Mater. Chem. A. 5 (2017) 24371.
[11] X. Kong, A.P. Kulkarni, S.A. Jenekhe, Macromolecules 36 (2003) 8992.
[12] A.A. Golriz, T. Kaule, M.B. Untch, K. Kolman, R. Berger, J.S. Gutmann, ACS Appl. Mater. Interfaces 5 (2013) 2485.
[13] F. Fungo, S.A. Jenekhe, A.J. Bard, Chem. Mater. 15 (2003) 1264.
[14] T.-T. Truong, G.W. Coates, H.D. Abruña, Chem. Commun. 51 (2015) 14674.
[15] H. Yang, D.O. Wipf, A.J. Bard, J. Electroanal. Chem. 331 (1992) 913.
[16] T. Mizoguchi, R.N. Adams, J. Am. Chem. Soc. 84 (1962) 2058.
[17] P. Ruiz-Castillo, S.L. Buchwald, Chem. Rev. 116 (2016) 12564.
[18] J.F. Hartwig, Synlett 0 (2006) 1283.
[19] R.A. Singer, J.P. Sadighi, S.L. Buchwald, J. Am. Chem. Soc. 120 (1998) 213.
[20] X.-X. Zhang, J.P. Sadighi, T.W. Mackewitz, S.L. Buchwald, J. Am. Chem. Soc. 122 (2000) 7606.
[21] B.M. Peterson, D. Ren, L. Shen, Y.-C.M. Wu, B. Ulgut, G.W. Coates, H.D. Abruña, B.P. Fors, ACS Appl. Energy Mater. 1 (2018) 3560.
[22] H. Etori, T. Kanbara, T. Yamamoto, Chem. Lett. 23 (1994) 461.
[23] P. Nguyen, P. Gómez-Elipe, I. Manners, Chem. Rev. 99 (1999) 1515.
[24] K. Naka, T. Uemura, Y. Chujo, Macromolecules 33 (2000) 6965.
[25] R. Rulkens, A.J. Lough, I. Manners, J. Am. Chem. Soc. 116 (1994) 797.
[26] R. Rulkens, A.J. Lough, I. Manners, S.R. Lovelace, C. Grant, W.E. Geiger, J. Am. Chem. Soc. 118 (1996) 12683.
[27] B.P. Fors, D.A. Watson, M.R. Briscoe, S.L. Buchwald, J. Am. Chem. Soc. 130 (2008) 13552.
[28] N.C. Bruno, M.T. Trudge, S.L. Buchwald, Chem. Sci. 4 (2013) 916.
[29] D. Maiti, B.P. Fors, J.L. Henderson, Y. Nakamura, S.L. Buchwald, Chem. Sci. 2 (2011) 57.
[30] T. Kinzel, Y. Zhang, S.L. Buchwald, J. Am. Chem. Soc. 132 (2010) 14073.
[31] D. Wei, C. Kvarnström, T. Lindfors, L. Kronberg, R. Sjöholm, A. Ivaska, Synth. Met. 156 (2006) 541.
[32] D.A. Buttry, M.D. Ward, Chem. Rev. 92 (1992) 1355.
[33] R. Borjas, D.A. Buttry, Chem. Mater. 3 (1991) 872.
[34] A.R. Hillman, D.C. Loveday, S. Bruckenstein, Langmuir 7 (1991) 191.
[35] J. John, K.M. Hugar, J. Rivera-Meléndez, H.A. Kostalik, E.D. Rus, H. Wang, G.W. Coates, H.D. Abruña, J. Am. Chem. Soc. 136 (2014) 5309.